Chemistry & Biology
Article

Identification of Polyoxometalates as Nanomolar Noncompetitive Inhibitors of Protein Kinase CK2

Renaud Prudent,[1] Virginie Moucadel,[1] Béatrice Laudet,[1] Caroline Barette,[2] Laurence Lafanechère,[2] Bernold Hasenknopf,[3,*] Joaquim Li,[3,4] Sébastian Bareyt,[3,4] Emmanuel Lacôte,[4] Serge Thorimbert,[4] Max Malacria,[4] Pierre Gouzerh,[3] and Claude Cochet[1,*]
[1]Laboratoire de Transduction du Signal
[2]Centre de Criblage pour Molécules Bio-Actives (CMBA)
Institut de Recherche en Technologies et Sciences pour le Vivant, CEA, 17 Rue des Martyrs 38054 Grenoble, France
[3]Laboratoire de Chimie Inorganique et Matériaux Moléculaires (UMR CNRS 7071)
[4]Laboratoire de Chimie Organique (UMR CNRS 7611)
UPMC Univ. Paris 06, Institut de Chimie Moléculaire (FR 2769), 4 Place Jussieu, 75005 Paris, France
*Correspondence: bernold.hasenknopf@upmc.fr (B.H.), ccochet1@cea.fr (C.C.)
DOI 10.1016/j.chembiol.2008.05.018

SUMMARY

Protein kinase CK2 is a multifunctional kinase of medical importance that is dysregulated in many cancers. In this study, polyoxometalates were identified as original CK2 inhibitors. $[P_2Mo_{18}O_{62}]^{6-}$ has the most potent activity. It inhibits the kinase in the nanomolar range by targeting key structural elements located outside the ATP- and peptide substrate-binding sites. Several polyoxometalate derivatives exhibit strong inhibitory efficiency, with IC_{50} values $\leq$ 10 nM. Furthermore, these inorganic compounds show a striking specificity for CK2 when tested in a panel of 29 kinases. Therefore, polyoxometalates are effective CK2 inhibitors in terms of both efficiency and selectivity and represent nonclassical kinase inhibitors that interact with CK2 in a unique way. This binding mode may provide an exploitable mechanism for developing potent drugs with desirable properties, such as enhanced selectivity relative to ATP-mimetic inhibitors.

INTRODUCTION

Dysregulation of signal transduction pathways underlies many diseases, including cancers. These pathways are rich in protein kinases. Perturbation of these protein kinase-mediated regulatory networks can lead to various disease states that might be amenable to therapeutic intervention. Thus, protein kinases are major therapeutic targets, and several kinase inhibitors have demonstrated powerful clinical activity in tumors in which the target kinase is deregulated (Bogoyevitch and Fairlie, 2007).

Protein kinase CK2 (formerly known as Casein Kinase II) is a multifunctional serine/threonine kinase that plays critical roles in cell growth, cell differentiation, apoptosis, and oncogenic transformation (Ahmed et al., 2002; Litchfield, 2003). CK2 is involved in animal development and oncogenesis, where it has been found to be dysregulated. Its dual function in promoting cell growth and suppressing apoptosis confers a relevant oncogenic potential (Tawfic et al., 2001). Association of aberrant CK2 expression with unfavorable prognostic markers in prostate cancer (Laramas et al., 2007) and in acute myeloid leukemia (Kim et al., 2007) confers to CK2 the status of relevant pathophysiological target, thus supporting the identification and the characterization of chemical inhibitors (Pagano et al., 2006). Hence, numerous CK2 inhibitors appeared over the past few years in the literature: halogenated compounds TBB (4,5,6,7-tetrabromo-1*H*-benzotriazole) and DMAT (2-dimethylamino-4,5,6,7-tetrabromo-1*H*-benzimidazole) (Sarno et al., 2003; Pagano et al., 2004), condensed polyphenolic derivatives (anthraquinones, xanthenones, fluorenones, and coumarins) (Meggio et al., 2004), and a 7-substituted indoloquinazoline compound (Vangrevelinghe et al., 2003) have been reported to inhibit CK2 in the micromolar range. All of these inhibitors are aromatic organic compounds and behave as ATP mimetics, highlighting the necessity to search among new classes of molecules for new inhibitors. Indeed a recent report has identified a platinum complex as a nanomolar inhibitor of glycogen synthase kinase 3 (GSK-3α) (Williams et al., 2007). However, the compound also binds to the ATP-binding site. Screening of very diverse libraries is a way to find new active compounds. Therefore, we used this strategy to develop non-ATP-competitive CK2 inhibitors.

Using high-throughput screening of highly diverse chemical libraries, we have identified inorganic CK2 inhibitors, namely, polyoxometalates (POMs). These are aggregates of early-transition metal ions (mainly M = V^V, Mo^{VI}, or W^{VI}) and oxo ligands (Pope, 2003), which are formed in solution by condensation reactions of the oxo anion MO_4^{n-}. Depending on the boundary conditions (temperature, pH, and composition of the solution), many different structures arise. These nanometer-sized compounds bear multiple negative charges distributed over the whole surface, thus keeping the charge density relatively low. Figure 1 shows typical examples of POMs relevant to this work.

Antiviral, antitumoral, and antibiotic activities have been reported for several POMs (Yamase, 2005; Hasenknopf, 2005; Rhule et al., 1998). Although the molecular target of the POM is generally unknown, several papers report detailed study of the interaction between POMs and a given protein (Hervé

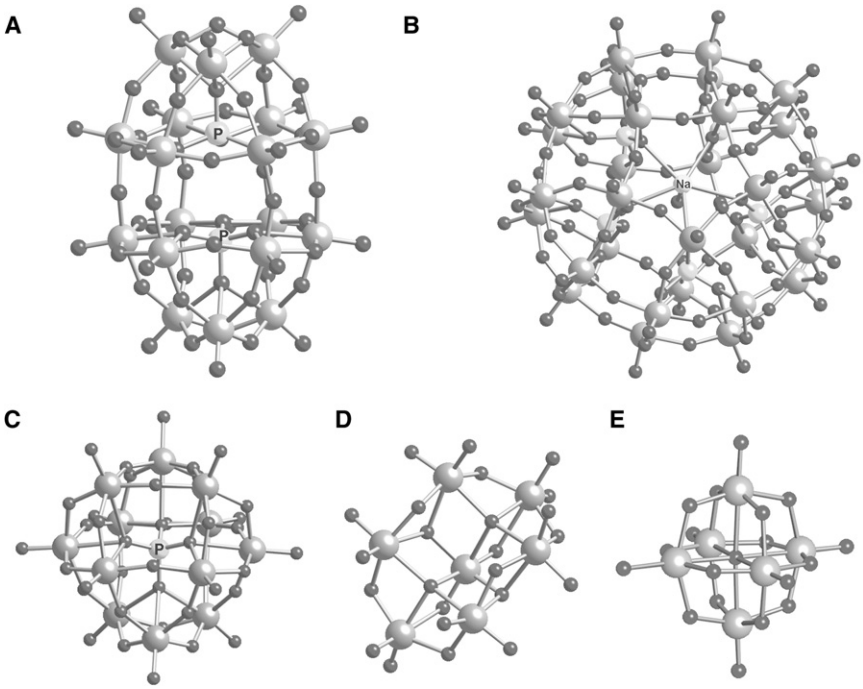

Figure 1. Ball-and-Stick Representation of Typical Polyoxometalates
(A) Dawson structure, α-$[P_2W_{18}O_{62}]^{6-}$.
(B) Preyssler structure, $[NaP_5W_{30}O_{110}]^{14-}$.
(C) Keggin structure, α-$[PW_{12}O_{40}]^{3-}$.
(D) Heptamolybdate, $[Mo_7O_{24}]^{6-}$.
(E) Lindqvist structure, $[Mo_6O_{19}]^{2-}$.
W, Mo = large light-gray spheres, O = small dark-gray spheres, other elements noted on the figure.

et al., 1983; Hill et al., 1990; Crans, 1993; Sarafianos et al., 1996; Judd et al., 2001). Binding of POMs to *Escherichia coli* DNA polymerase (Hervé et al., 1983), to HIV-1 reverse transcriptase (Sarafianos et al., 1996), and to protease (Judd et al., 2001) was established. In the former two cases, the polyanionic POM binds to the DNA-binding site, whereas, in the latter case, it binds outside the active site. Several classic POMs bind to Basic Fibroblast Growth Factor, a globular heparin-binding polypeptide, presumably at a cationic pocket. Then, the structure of the protein is affected, which results in a stabilizing effect relative to the free protein (Wu et al., 2005; Sun et al., 2004). Decavanadate has a high affinity for myosin and the sarcoplasmic reticulum calcium pump, and, in some biological systems, the effects of vanadium can be related to the presence of decavanadate (Aureliano and Gandara, 2005). Decavanadate was also reported to be an antisubstrate inhibitor of cAMP-dependent protein kinase (Pluskey et al., 1997). Polyoxotungstates were identified as potent inhibitors of ectonucleoside triphosphate diphosphohydrolase, and some displayed a useful selectivity pattern (Müller et al., 2006). POMs are also known to selectively precipitate some types of proteins, for instance the prion protein (Lee et al., 2005).

RESULTS AND DISCUSSION

High-Throughput Identification of Polyoxometalates

The National Cancer Institute (NCI) Diversity Set (1985 compounds) and the Mechanistic Diversity Set (879 compounds) were screened at concentrations of 15 μM by using an in vitro kinase assay. A secondary screen was performed at concentrations of 1.5 μM by using a standard radioactive kinase assay with high ATP concentrations (100 μM; K_m for ATP of recombinant CK2, 25 μM) to increase the probability of isolating non-ATP-competitive compounds. POMs were identified among active hits. We therefore investigated that class more closely by testing a series of POMs (see Table S1 available online).

The highest inhibition was observed for $K_6[P_2Mo_{18}O_{62}]$, a phosphomolybdate with the Dawson structure (Figure 1A). Derivatives of the Dawson structure showed moderate to high inhibition of CK2. The Preyssler anion $K_{14}[NaP_5W_{30}O_{110}]$ (Figure 1B) also had good activity as an inhibitor, as does the giant phosphotungstate $K_{28}Li_5H_7[P_8W_{48}O_{184}]$. Smaller POMs such as Keggin derivatives $[XM_{12}O_{40}]^{n-}$ (Figure 1C), the heptamolybdate $[Mo_7O_{24}]^{6-}$ (**1D**), or the Lindqvist molybdate $[Mo_6O_{18}]^{2-}$ (**1E**), were less active.

Structure-Activity Relationship of POMs

To better quantify the inhibitory effect of POMs, and to attempt to correlate it to structural or compositional features, we determined the IC_{50} value of a series of POMs. We included in this series a number of Preyssler structures with different lanthanide ions, Dawson structures with lanthanides or organotin substituents, and Keggin ions with organotin substituents in order to compare the effects of structures (Preyssler, Dawson, Keggin) and composition/functionalization (lanthanides, organotin groups). We also included $(NH_4)_{18}[NaSb_9W_{21}O_{86}]$ (HPA-23) and one of its lanthanide derivatives as additional examples of a highly charged, very large POM. Our results are presented in Table 1.

It can be concluded that the POM structure mainly determines its inhibitory effect. Data indicate that the inhibitory efficiency increases with the size and the charge of the administered POM. Small Keggin ions are inactive, larger Dawson compounds are moderately active, and the largest and most charged Preyssler ions are the best subgroup of inhibitors. Derivatives within the same POM family are of comparable activity. It is not surprising to find more pronounced differences between the different Dawson compounds, where the modifications are located at the periphery of the framework, compared to the series of Preyssler ions, where the different lanthanide ions are buried in the center of the structure. There are no clear trends to explain the variation of activity caused by the side chain modifications among the organotin-substituted Dawson POMs. However, the organic groups did not include any particular protein-recognition motif. More designed organic-inorganic hybrids might have an enhanced activity, provided we get a clear picture of the POM-CK2 interaction.

Table 1. Inhibitory Power of POMs toward CK2α

Formula	M ($g \cdot mol^{-1}$)	IC_{50} (nM)	Type
$K_6[P_2Mo_{18}O_{62}]$	3015	1.4	Dawson
$K_{12}[LuP_5W_{30}O_{110}]$	8076	1	Preyssler
$K_{12}[SmP_5W_{30}O_{110}]$	8051	3	Preyssler
$K_{12}[YbP_5W_{30}O_{110}]$	8174	3	Preyssler
$\{N(C_4H_9)_4\}_7$ α_1-$[P_2W_{17}O_{61}\{Sn(CH_2)_2COOH\}]$	6084	3.5	Dawson (organic derivative, belt)
$K_{12}[YP_5W_{30}O_{110}]$	7990	5	Preyssler
$[\{N(C_4H_9)_4\}_7$ α_2-$[P_2W_{17}O_{61}\{Sn(CH_2)_2CHO\}]$	6068	7.5	Dawson (organic derivative, cap)
$(NH_4)_{18}[NaSb_9W_{21}O_{86}]$	6681	8	Giant POM (HPA-23)
$\{N(C_4H_9)_4\}_7$ α_2-$[P_2W_{17}O_{61}\{Sn(CH_2)_2CONBn_2\}]$	6060	11	Dawson (organic derivative, cap)
$\{N(C_4H_9)_4\}_7$ α_2-$[P_2W_{17}O_{61}\{Sn(CH_2)_2COOH\}]$	4849	13	Dawson (organic derivative, cap)
$(NH_4)_{16}[EuSb_9W_{21}O_{86}]$	6810	13	Giant POM (HPA-23 lanthanide derivative)
$\{N(C_4H_9)_4\}_3$ $[PW_{12}O_{40}]$	3604	60	Keggin
$\{N(C_4H_9)_4\}_7$ α_1-$[P_2W_{17}O_{61}\{Sn(CH_2)_2CONHBn_2\}]$	6232	70	Dawson (organic derivative, belt)
$K_{21}H_4[EuAs_4W_{40}O_{140}]$	10872	70	Giant POM
$\{N(C_4H_9)_4\}_7$ α_1-$[P_2W_{17}O_{61}\{Sn(CH_2)_2CONHCH_2$-*m*-$C_6H_4CH_2NHBoc\}]$	6271	>7	Dawson (organic derivative, belt)
$K_7[\alpha_1$-$YbP_2W_{17}O_{61}]$	4681	>7	Dawson (lanthanide derivative, belt)
$\{N(C_4H_9)_4\}_7$ α_1-$[P_2W_{17}O_{61}\{Sn(CH_2)_2CO$-(L-Tyr)-$O^tBu\}]$	6273	>7	Dawson (organic derivative, belt)
$\{N(C_4H_9)_4\}_7$ α_1-$[P_2W_{17}O_{61}\{Sn(CH_2)_2CO$-(Gly)-$O^tBu\}]$	6166	>7	Dawson (organic derivative, belt)
$K_7[\alpha_1$-$EuP_2W_{17}O_{61}]$	4660	>7	Dawson (lanthanide derivative, belt)
$K_7[\alpha_1$-$SmP_2W_{17}O_{61}]$	4659	>7	Dawson (lanthanide derivative, belt)
$K_7[\alpha_1$-$LaP_2W_{17}O_{61}]$	4647	>70	Dawson (lanthanide derivative, belt)
$\{N(C_4H_9)_4\}_4$ α-$[PW_{11}O_{39}\{Sn(CH_2)_2CONBn_2\}]$	4018	>70	Keggin (organic derivative)
$\{N(C_4H_9)_4\}_4$ α-$[PW_{11}O_{39}\{Sn(CH_2)_2CONC_5H_{10}\}]$	3906	>70	Keggin (organic derivative)
$\{N(C_4H_9)_4\}_4$ α-$[PW_{11}O_{39}\{Sn(CH_2)_2CONHCy\}]$	3920	>70	Keggin (organic derivative)
$\{N(C_4H_9)_4\}_4$ α-$[PW_{11}O_{39}\{Sn(CH_2)_2CONHBn\}]$	3928	>70	Keggin (organic derivative)
$\{N(C_4H_9)_4\}_4$ α-$[PW_{11}O_{39}\{Sn(CH_2)_2CONH$-*p*-$C_6H_4OMe\}]$	3944	>70	Keggin (organic derivative)
$\{N(C_4H_9)_4\}_4$ α-$[PW_{11}O_{39}\{Sn(CH_2)_2CONHCH_2$-*m*-$C_6H_4CH_2NHBoc\}]$	4057	>70	Keggin (organic derivative)
$K_7[PW_{11}O_{39}]$	3320	1000	Lacunary Keggin
$\{N(C_4H_9)_4\}_3$ $[PMo_{12}O_{40}]$	2548	>50	Keggin
$H_3[PMo_{12}O_{40}]$	1829	>50 (1000)	Keggin

For IC_{50} determination, SEMs never exceeded 10%. All of the Preyssler structures exhibited a remarkable in vitro inhibitory power toward CK2, with IC_{50} values $\leq$ 5 nM (calculated at 100 μM ATP). This property is not related to the presence of lanthanides, but to the POM framework, as the lanthanide-Dawson structures are less active. In turn, comparison of Dawson and Keggin ions with the same organic side chain indicates that the moderate activity of the Dawson derivatives is mostly related to their underlying inorganic structure. Keggin ions with equivalent organic groups are much less active. HPA-23 has a fairly low IC_{50} value, only slightly higher than the Preyssler compounds and in line with the most active Dawson structures.

POM structures are known to depend on concentration, pH, and buffer characteristics (Pope, 2003). Utmost care therefore has to be taken when establishing a structure-activity relationship for POMs because the precise structures present at the low concentrations of biological experiments are difficult to determine (Hill et al., 1990). The Preyssler anions are known to be very stable in neutral to slightly basic aqueous solutions, and the organotin-substituted phosphotungstates are kinetically stable at neutral pH for the time of the present measurements. These POMs are likely to be intact during the kinase assays. As the lanthanide phosphotungstates with Dawson structure have similar activity as the organotin Dawson phosphotungstates, they are probably also intact during the assay. At least, they are not hydrolyzed into small fragments, as smaller POMs are inactive. In this context, it is surprising to find the Dawson POM $[P_2Mo_{18}O_{62}]^{6-}$ as the most active compound, because this POM is known to be hydrolyzed very rapidly at neutral pH. We confirmed rapid hydrolysis in the buffer solution by UV-vis spectroscopy ($t_{1/2} < 5$ min at 30 μM). However, the components MoO_4^{2-} and PO_4^{3-}, when tested individually or in combination, are inactive. This intriguing activity of $[P_2Mo_{18}O_{62}]^{6-}$ prompted us to investigate this compound further.

$[P_2Mo_{18}O_{62}]^{6-}$ as a Selective Kinase Inhibitor

We examined the inhibitory effects of $[P_2Mo_{18}O_{62}]^{6-}$ on a panel of 29 recombinant serine/threonine and tyrosine kinases involved in cell signaling (Table S2). At 100 nM, $[P_2Mo_{18}O_{62}]^{6-}$ inhibited CK2 by more than 95%, but it had almost no effect on the other protein kinases tested, apart from GSK3β and c-Src. However, the IC_{50} values for these kinases (GSK3β, 27 nM;

c-Src, 77 nM) were more than one to two orders of magnitude higher than the IC_{50} value determined for CK2 (1.4 nM). Thus, for these different kinases, $[P_2Mo_{18}O_{62}]^{6-}$ shows greater than 40-fold selectivity for CK2 over 28 other kinases tested. By comparison to other published CK2 inhibitors used as benchmarks (Table S3), we can conclude that $[P_2Mo_{18}O_{62}]^{6-}$ is one of the most selective CK2 inhibitors.

Mechanism of CK2 Inhibition by $[P_2Mo_{18}O_{62}]^{6-}$

The low IC_{50} exhibited by the Preyssler and Dawson structures for CK2 were even lower than the CK2 molarity in the assay (50 nM). This observation led us to explore more thoroughly the mechanism of action of CK2 inhibition by POMs. POMs often induce protein aggregation through multivalent electrostatic interactions (Lee et al., 2005; Tajima, 2004). Thus, recombinant CK2α was incubated with increasing concentrations of $[P_2Mo_{18}O_{62}]^{6-}$ in the assay medium. After ultracentrifugation, a western blot analysis of the supernatants did not show any evidence for POM-induced precipitation of CK2α for concentrations below 10 μM (Figure S1). Other possible mechanisms of inhibition consist of either complexation of several CK2 molecules by one $[P_2Mo_{18}O_{62}]^{6-}$ or fragmentation of the POM into several inhibitory moieties. To explore the former hypothesis, we carried out sucrose density gradient sedimentation analysis (Valero et al., 1995).

Recombinant CK2α was analyzed under catalytic conditions by velocity sedimentation through sucrose gradients containing different $[P_2Mo_{18}O_{62}]^{6-}$ concentrations. In the absence of POM, the enzyme sedimented as a single peak with an approximate 3.5 S sedimentation coefficient corresponding to its monomeric form (Figure S2). This sedimentation behavior was not affected by the presence of $[P_2Mo_{18}O_{62}]^{6-}$ at concentrations up to 100 nM. Aggregated forms of CK2α sedimenting at the bottom of the tube were only detected in the presence of 1 μM $[P_2Mo_{18}O_{62}]^{6-}$. Thus, we can conclude that in the presence of nanomolar concentrations of POM, CK2α does not form oligomeric structures.

We propose that the powerful inhibition of CK2 by POM could be due, at least for $[P_2Mo_{18}O_{62}]^{6-}$, to fragments of this compound. This would be consistent with the fact that phosphomolybdates undergo multiple equilibria depending on medium composition (Pettersson et al., 1986). Therefore, we tested the inhibitory activity of $[P_2Mo_{18}O_{62}]^{6-}$ after prior incubation in the kinase assay buffer (Figure S3). One should keep in mind that UV-vis spectroscopy showed fast hydrolysis of $[P_2Mo_{18}O_{62}]^{6-}$ under these conditions. It was observed that the inhibitory activity of $[P_2Mo_{18}O_{62}]^{6-}$ vanished after prior incubation in buffer, but remained unchanged after 30 min of incubation at 25°C in a BSA-containing assay medium. These results give clear evidence that the active form of the POM is a particular protein-stabilized product, since hydrolysis in protein-free buffer leads to inactive compounds. This is reminiscent of the POM fragments identified in the Mo/W storage protein from *Azotobacter vinelandii*. (Schemberg et al., 2007) Some of those fragments also occur only in the protein environment and cannot be isolated as free entities. It is thus not possible to use speciation data of phosphomolybdates in water (Pettersson et al., 1986; Himeno et al., 1999; Briand et al., 2002) to determine the active structure. The protein-stabilized form of the POM issued from $[P_2Mo_{18}O_{62}]^{6-}$ might or might not be different in BSA and CK2, but both proteins block the total hydrolysis of $[P_2Mo_{18}O_{62}]^{6-}$, and the BSA-stabilized form also inhibits CK2.

Spectroscopic studies to establish the structures of the active CK2-bound form of POMs have been unsuccessful so far. It has also not been possible to analyze the complex POM-CK2 by ESI-MS, since the protein was not in its native form in buffer solutions compatible with that technique. However, the fact that the rapid hydrolysis of $[P_2Mo_{18}O_{62}]^{6-}$ appears to be correlated with the loss of activity highlights the importance of a particular POM composition and structure that can undergo specific interactions with CK2. As we cannot give the formula of the active form, we continue to use the formula of the administered form, $[P_2Mo_{18}O_{62}]^{6-}$, in the subsequent sections.

To define the biochemical mechanism of action of $[P_2Mo_{18}O_{62}]^{6-}$, we next examined the effects of increasing concentrations of ATP or peptide substrate on the inhibitory activity of the compound by using steady-state analysis. The values from individual samples were analyzed and plotted as a function of inhibitor concentration. Lineweaver-Burk inhibition plots showed that, in the presence of a saturating peptide substrate concentration (600 μM), $[P_2Mo_{18}O_{62}]^{6-}$ can bind to either the CK2-peptide substrate complex (K_i = 7 nM) or the CK2-ATP-peptide substrate complex (K_i = 5.3 nM), suggesting a mixed inhibition of CK2 by $[P_2Mo_{18}O_{62}]^{6-}$ with respect to ATP (Figure 2A).This indicates that $[P_2Mo_{18}O_{62}]^{6-}$ is not an ATP site-directed inhibitor. The effects of increasing concentrations of peptide substrate on the inhibitory activity of the compound in the presence of saturating ATP concentration (100 μM) was examined (Figure 2B). Steady-state kinetic analysis reveals that the apparent K_m for peptide substrate is invariant, a characteristic of noncompetitive inhibition, $[P_2Mo_{18}O_{62}]^{6-}$ being able to bind equally well to the CK2-ATP or the CK2-ATP-peptide substrate complex (K_i = 6.5 nM). This behavior provides evidence that $[P_2Mo_{18}O_{62}]^{6-}$ is not a peptide substrate site-directed inhibitor.

Binding Site of $[P_2Mo_{18}O_{62}]^{6-}$

We next searched for a putative POM-binding site on CK2α by using four complementary approaches: (1) kinase assay with CK2 holoenzyme, (2) affinity chromatography with an immobilized POM, (3) trypsin proteolysis, and (4) site-directed mutagenesis.

First, a CK2 kinase assay was performed with either CK2α alone or reconstituted CK2 holoenzyme ($CK2\alpha_2/CK2\beta_2$) (Valero et al., 1995) to determine the influence of the regulatory CK2β subunit on the inhibitory activity of $[P_2Mo_{18}O_{62}]^{6-}$. Similar IC_{50} values were obtained, indicating that the binding of CK2β on CK2α does not affect the kinase sensitivity for the inhibitor, thus ruling out the involvement of the CK2α/CK2β interface in the interaction (Figure 3).

To understand the precise nature of the interactions of POMs with CK2α, we next performed binding assays in which recombinant CK2α was incubated with a biotinylated Keggin POM (BK). A CK2 kinase assay performed in the presence of BK showed that this functionalized POM inhibits CK2α through a similar mechanism as the Dawson ion $[P_2Mo_{18}O_{62}]^{6-}$ (mixed inhibition with respect to ATP) (Figure S4). Recombinant CK2α was incubated with BK or biotinylated CK2β immobilized on streptavidine-Sepharose beads. The results presented in Figure 4A indicate the presence of CK2α associated to the

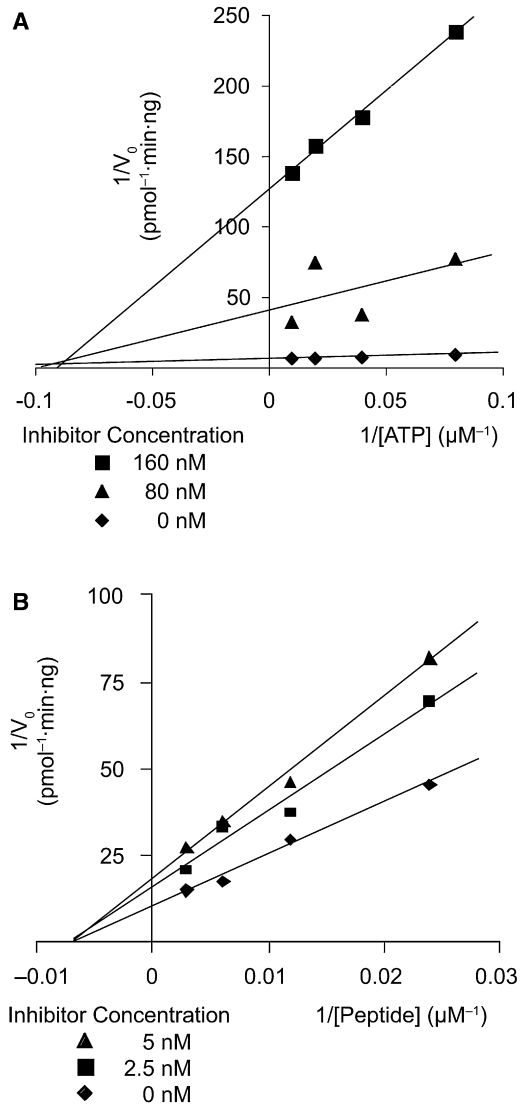

Figure 2. Steady-State Kinetic Analysis of $[P_2Mo_{18}O_{62}]^{6-}$/CK2 Complexation

(A and B) CK2 activity was determined as described in the Experimental Procedures either in the absence or in the presence of the indicated $[P_2Mo_{18}O_{62}]^{6-}$ concentrations. (A) Steady-state kinetic analysis carried out with a saturating peptide substrate concentration (600 μM). (B) Steady-state kinetic analysis carried out with a saturating ATP concentration (100 μM). The data represent means of experiments run in triplicate, with SEM never exceeding 10%.

beads loaded with BK or CK2β and a decrease of CK2 activity in the corresponding supernatants. Thus, like with CK2β, a high-affinity interaction was detected between the Keggin compound and CK2α. This fact allowed us to perform affinity chromatography on immobilized BK in the presence of CK2β, ATP, CK2 peptide substrate, and TBB (Figure 4B). CK2α was not displaced from the BK resin by a stoichiometric amount of CK2β (in accordance with the similar IC_{50} values of POM for the CK2 holoenzyme and for the isolated CK2α). In addition, neither ATP nor TBB nor a CK2 peptide substrate interfered with the ability of CK2α to bind to the immobilized POM.

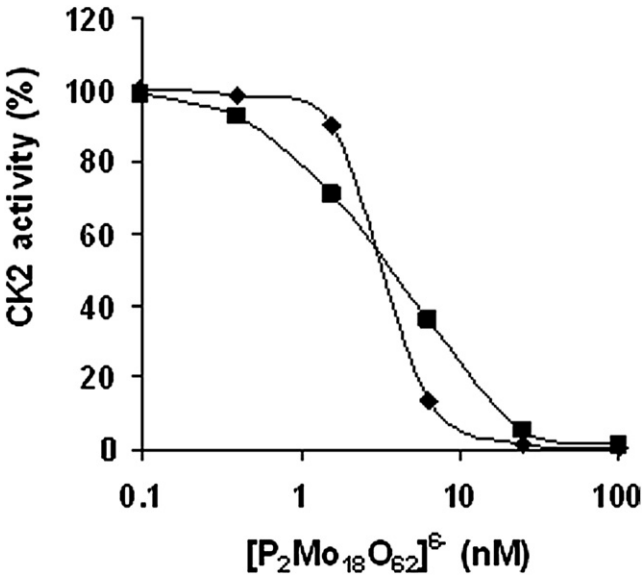

Figure 3. Dose-Dependent Inhibition of Two Forms of CK2 by $[P_2Mo_{18}O_{62}]^{6-}$

Activity assays of the isolated CK2 catalytic subunit (diamonds) or the CK2 holoenzyme (squares) were performed as described in Experimental Procedures in the presence of increasing $[P_2Mo_{18}O_{62}]^{6-}$ concentrations. The data represent means of two independent experiments.

Collectively, these data indicate that the POM likely binds outside the CK2α/CK2β interface and the ATP/peptide-binding pocket.

Next, samples of CK2α complexed with $[P_2Mo_{18}O_{62}]^{6-}$ were subjected to partial proteolysis in the presence of trypsin, and the resultant proteolytic fragments were separated by SDS-PAGE. The results depicted in Figure 5A show that whereas CK2α was almost completely degraded after 30 min, the CK2α-$[P_2Mo_{18}O_{62}]^{6-}$ complex led to the generation of two low-molecular weight fragments (6.3 and 5.6 kDa) that were resistant to trypsin degradation for up to 60 min. Under similar conditions, trypsin-induced degradation of BSA was not affected by the presence of $[P_2Mo_{18}O_{62}]^{6-}$ (not shown). Thus, the two protein fragments that are protected from degradation owing to a high-affinity interaction of $[P_2Mo_{18}O_{62}]^{6-}$ with CK2α may represent minimal interacting domains. Therefore, these fragments were extracted from the SDS-PAGE gel and subjected to amino acid sequencing analysis. This analysis revealed that the 6.3 kDa fragment (residues 22–68) contains the N-terminal domain and three β strands (β1, β2, and β3). Strands β1 and β2 are the major contacts with the CK2β dimer at the interface. This region also displays the glycine-rich loop (Figure 5B). (Niefind et al., 2001) The 5.6 kDa fragment (residues 192–244) consists of the activation segment and two α helices (αF and αG). Thus, these protected fragments may contain putative inhibitor binding site(s).

Finally, to investigate whether introducing mutations into helix C and the activation segment affects the $[P_2Mo_{18}O_{62}]^{6-}$ inhibitory potency, we mutated several residues located in or close to the identified trypsin resistant fragments (Figure 5C). $[P_2Mo_{18}O_{62}]^{6-}$ was tested for its ability to inhibit the activity of wild-type (WT) and K49A/F54L, K74A, and R191A CK2α mutants

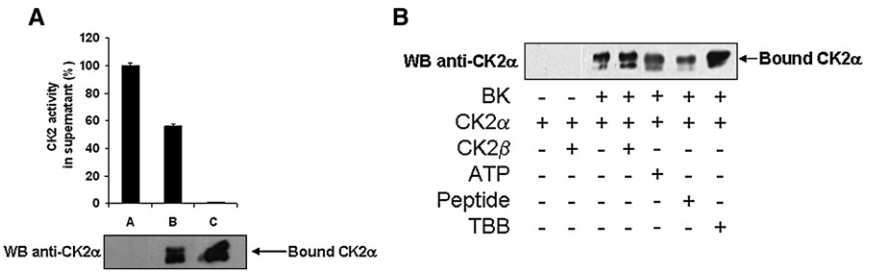

Figure 4. Affinity Chromatography Experiments with Biotinylated POM

(A–B) (A) Recombinant CK2α binds to Biotin-Keggin polyoxometalate. CK2α (240 ng) was incubated with (A) streptavidine-Sepharose beads alone or with streptavidine-Sepharose beads loaded with (B) biotinylated Keggin or biotinylated CK2β. After centrifugation of the beads, CK2 activity was assayed in the supernatants, and the presence of CK2α associated to the beads was detected by western blot. (B) Binding specificity of Biotin-Keggin polyoxometalate on CK2α. Sepharose-immobilized Biotin-Keggin polyoxometalate was incubated with CK2α (240 ng) in the absence or presence of a stoichiometric amount of CK2β, 100 μM ATP, 100 μM CK2 peptide substrate, or 100 μM TBB. After extensive washing, the bound protein was resolved by SDS-PAGE and was immunodetected with anti-CK2α.

(Figure 5D). It was observed that the sensitivity of these CK2α mutants to $[P_2Mo_{18}O_{62}]^{6-}$ inhibition was significantly affected, resulting in a shift to a higher IC_{50}. Conversely, other mutations in the identified protected fragments (K198A) or outside these fragments (R80A) were without effect (not shown). Thus, specific mutations in key structural elements like the glycine-rich loop, helix C, and activation segment weaken the CK2α sensitivity to $[P_2Mo_{18}O_{62}]^{6-}$ inhibition.

Cell Assay

Pharmacokinetic characteristics of POMs are critical issues for developing these compounds as chemotherapeutic agents. Therefore, we investigated whether $[P_2Mo_{18}O_{62}]^{6-}$ could inhibit CK2 in living cells by using a cellular CK2 activity assay. HeLa cells expressing a CK2 peptide substrate reporter were incubated with TBB, $[P_2Mo_{18}O_{62}]^{6-}$, or DMSO as a control (Figure 6A). The cellular phosphorylation of the CK2 substrate reporter was strongly inhibited in TBB-treated cells. In contrast, this phosphorylation was not affected in cells incubated with $[P_2Mo_{18}O_{62}]^{6-}$. This could result from the high charge of the POM framework that might prevent their delivery inside the cells or by degradation of the active compound in the cellular environment. To determine whether $[P_2Mo_{18}O_{62}]^{6-}$ inhibits CK2 in a complex cellular protein mixture, we used whole brain tissue lysates as a source of CK2 that potentially conserves, at least in part, the physiological environment of the kinases. This cell-free system may be seen as a compromise between living cells and recombinant CK2, as it preserves, to some extent, the biochemical context of the target, but is not dependent on the cell permeability of the POM. Brain extracts were incubated with increasing concentrations of $[P_2Mo_{18}O_{62}]^{6-}$, and CK2 activity was assayed. It was observed that $[P_2Mo_{18}O_{62}]^{6-}$ inhibited the CK2 activity in a dose-dependent manner with an IC_{50} value of 0.6 μM (Figure 6B). Next, we examined the effect of $[P_2Mo_{18}O_{62}]^{6-}$ on the phosphorylation of endogenous CK2 substrates present in brain extracts. As CK2 is one of the few kinases using GTP as a phosphate donor, tissue extracts were incubated with [γ-^{32}P]GTP-$MgCl_2$ (Figure 6C). Under these experimental conditions, several phosphorylated proteins were detected. The phosphorylation of three of them was enhanced by the addition of

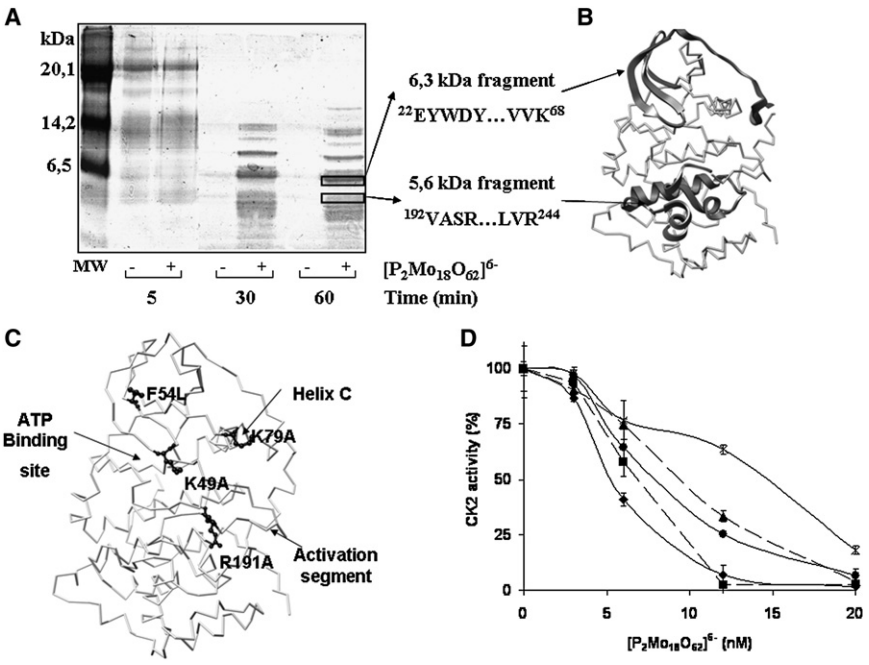

Figure 5. Localization of the $[P_2Mo_{18}O_{62}]^{6-}$ Binding Site

(A) Time course tryptic proteolysis of the $[P_2Mo_{18}O_{62}]^{6-}$-CK2α complex. $[P_2Mo_{18}O_{62}]^{6-}$-CK2α complexes were purified by gel-exclusion chromatography and subjected to tryptic proteolysis for the indicated time. The resultant proteolytic fragments were separated by SDS-PAGE. After completion of the tryptic proteolysis, the low-molecular weight 6.3 and 5.6 kDa fragments were extracted from the gel and sequenced by Edmann degradation.

(B) The crystal structure of CK2α (adapted from Niefind et al., 2001) and trypsin-resistant fragments (6.3 kDa, residues 22–68; 5.6 kDa, residues 192–244) are highlighted in dark gray.

(C) Model showing mutations within CK2α affecting $[P_2Mo_{18}O_{62}]^{6-}$ activity. Mutations K49A/F54L, K74A, and R191A are depicted in black balls and sticks in the CK2α ribbon.

(D) Inhibitory effect of $[P_2Mo_{18}O_{62}]^{6-}$ on WT (diamonds) and K49A/F54L (triangles), K74A (circles), and R191A (squares) CK2α mutants.

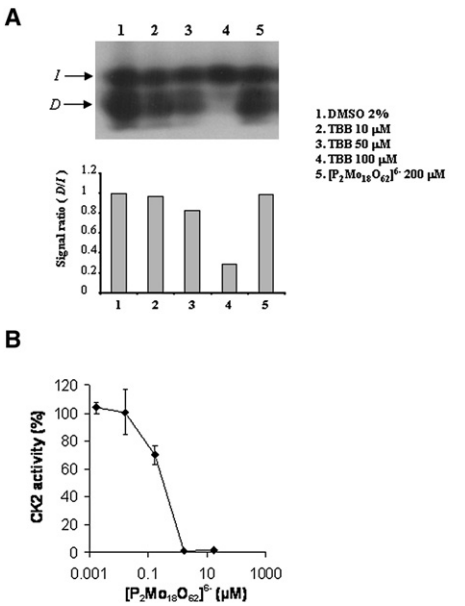

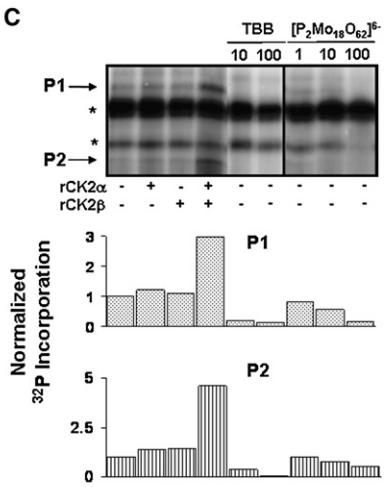

Figure 6. Inhibition of CK2 by $[P_2Mo_{18}O_{62}]^{6-}$ in a Cellular Environment

(A) Lack of CK2 inhibition by $[P_2Mo_{18}O_{62}]^{6-}$ in living cells. HeLa cells expressing a fusion construct consisting of several repeats of a CK2 peptide substrate fused to GFP were incubated for 48 hr with 100 μM TBB, $[P_2Mo_{18}O_{62}]^{6-}$, or an equivalent amount of DMSO as a control. Proteins from the cell extracts were resolved by native 12% PAGE and immunoblotted with anti-GFP. The CK2-dependent phosphorylated form of the CK2 peptide substrate reporter is indicated by the arrow.

(B) Inhibition of CK2 by $[P_2Mo_{18}O_{62}]^{6-}$ in a complex protein mixture. Murine brain extracts were incubated with increasing $[P_2Mo_{18}O_{62}]^{6-}$ concentrations (0.001–10 μM), and CK2 activity was assayed as described in Experimental Procedures. Each point is the mean of duplicate assays (variation is indicated by error bars) and designates CK2 activity expressed as a percentage of activity in the absence of compound.

(C) Inhibition of CK2 substrate phosphorylation in murine brain extracts by $[P_2Mo_{18}O_{62}]^{6-}$. Extracts were incubated with [γ-^{32}P]GTP-$MgCl_2$ in the absence or presence of recombinant CK2 subunits, 10 or 100 μM TBB, and 1–100 μM $[P_2Mo_{18}O_{62}]^{6-}$. Proteins were analyzed by SDS-PAGE, and phosphoproteins were visualized by autoradiography. The arrows show endogenous CK2 substrates. The asterisk indicates a protein substrate for a CK2-unrelated kinase.

recombinant CK2 and was strongly inhibited by TBB, indicating that they are potential CK2 substrates. The phosphorylation of these CK2 substrates was inhibited by $[P_2Mo_{18}O_{62}]^{6-}$ in a dose-dependent manner. This is combined evidence that $[P_2Mo_{18}O_{62}]^{6-}$ is a CK2 inhibitor in this cell-like environment.

SIGNIFICANCE

Mechanisms of action and cellular targets of POMs are poorly defined, with only few documented cases. (Hervé et al., 1983; Hill et al., 1990; Crans, 1993; Sarafianos et al., 1996; Judd et al., 2001; Mitsui et al., 2006; Müller et al., 2006; Hu et al., 2007). Our work reports that POMs are powerful nonclassical CK2 inhibitors, with $[P_2Mo_{18}O_{62}]^{6-}$ being one of the most potent and selective CK2 inhibitors. Recurrent features of biologically active POMs are their high charge and the large size of their framework. However, in our study, the active form is a protein-stabilized degradation product. Identification of this active product by crystallization of POM-CK2 complexes is underway.

The pharmacokinetic characteristics (distribution, clearance) of the POMs presented here make them very unlikely new drugs. Yet the design of functionalized POMs coupled to organic molecules that would tune the parameters might lead to viable candidates. In addition, the study of their original inhibition mode contributes to a better understanding of the functioning of CK2, which will allow for the design of new drugs with different chemical compositions, but similar inhibition profiles.

CK2 inhibition by $[P_2Mo_{18}O_{62}]^{6-}$ is a mixed inhibition with respect to ATP and a noncompetitive one toward the phosphoacceptor peptide substrate. Moreover, no differences in POM sensitivity between the isolated CK2α subunit and the holoenzyme were observed, and the POM-CK2 interaction was also not affected by ATP, TBB, or a CK2 peptide substrate. This indicates that the POM-binding site does not involve either the ATP/peptide-binding pocket or the CK2β-binding domain. (Niefind et al., 2001). Proteolytic degradation of the CK2α-inhibitor complex and site-directed mutagenesis revealed that inhibitor-interacting domains contain key structural elements like the activation segment. This segment is stabilized by contacts to the N-terminal region that maintain CK2 in an active state (Niefind et al., 2001; Sarno et al., 2002). Thus, docking of $[P_2Mo_{18}O_{62}]^{6-}$ to the activation segment may disrupt these contacts, locking CK2 in an inactive conformation. Biophysical experiments aiming at deciphering this unexpected inhibition mode are underway.

EXPERIMENTAL PROCEDURES

Polyoxometalates

The following POMs were prepared according to published procedures and were characterized by NMR and/or IR spectroscopy: $K_6[P_2Mo_{18}O_{62}]$ (Briand et al., 2002) (by using KCl instead of NH_4Cl); $\{N(C_4H_9)_4\}_7[P_2W_{17}O_{61}SnR]$ (R = organic side chain) (Bareyt et al., 2003, 2005); $\{N(C_4H_9)_4\}_4[PW_{11}O_{39}SnR]$ (Sazani and Pope, 2004; Bareyt et al., 2005); $K_7[LnP_2W_{17}O_{61}]$ (Ln = lanthanide) (Bartis et al., 1997); $K_7[PW_{11}O_{39}]$ (Contant, 1987); $Na_{17}[(P_2W_{15}O_{56})_2Co_4(H_2O)(OH)]$ (Ruhlmann et al., 2002); $K_6[P_2W_{18}O_{62}]$, $K_{12}H_2\alpha$-$[P_2W_{12}O_{48}]$, $K_{28}Li_5H_7[P_8W_{48}O_{184}]$, and $Na_{12}[P_2W_{15}O_{56}]$ (Contant, 1990); $\{N(C_4H_9)_4\}_5H_4[P_2Nb_3W_{15}O_{62}]$ and $K_8H[P_2V_3W_{15}O_{62}]$ (Hornstein and Finke, 2002); and $\{N(C_4H_9)_4\}_2[Mo_6O_{19}]$ (Klemperer, 1990). All other POMs were part of the National Cancer Institute (NCI) library or were commercially available and were used as received.

BK

$TBA_4[PW_{11}O_{39}\{SnCH_2CH_2CO$-*m*-$NHCH_2C_6H_4CH_2NH$-*d*-biotine$\}]$ was prepared by adapting our published procedure for coupling organic molecules

to organotin functionalized polyoxotungstates (Bareyt et al., 2005). The complete procedure and full characterization are given in the Supplemental Data.

In Vitro Kinase Assays

Human recombinant CK2α was expressed in *Escherichia coli* and purified to homogeneity as previously described (Heriche et al., 1997). CK2 assays were performed in a final assay volume of 18 μl containing 3 μl compound, 3 μl CK2α (20 ng), and a mixture containing 1 mM of the peptide substrate RRREDEESDDEE, 10 mM $MgCl_2$, and [γ-^{32}P]ATP. The final concentration of ATP was 100 μM. Assays were performed at room temperature for 5 min before termination by the addition of 60 μl 4% TCA. ^{32}P incorporation in the peptide substrate was determined as described previously (Filhol et al., 1991).

Screening of a Chemical Library

A library of low-molecular weight compounds was obtained from the NCI, Bethesda, Maryland. For more information, see http://dtp.nci.nih.gov. Automated screening of compounds from the Structural Diversity Set and the Mechanistic Diversity Set were performed at 1.5 and 15 μM in 96-well plates by using a TECAN Genesis robot (http://www-dsv.cea.fr/cmba). CK2 activity was assayed for 30 min at room temperature in a final volume of 30 μl containing 10 μl compounds or DMSO controls, 10 μl CK2α (50 ng), and 10 μl of a mixture containing the peptide substrate and ATP at a final concentration of 100 μM and 10 μM, respectively. The final concentration of DMSO in the enzyme assay was less than 3.33%. At the end of the reaction, the kinase activity was determined by using the luminescence-based Kinase-Glo assay (Promega) according to the manufacturer's recommendations and BMG's FLUOstar microplate reader. This assay relies on the use of ATP depletion as a read-out for kinase activity.

Velocity Sedimentation

Linear 5%–20% (w/v) sucrose gradients were prepared in the following buffer: 50 mM Tris-HCl (pH 7.4), 150 mM NaCl, 20 mM $MgCl_2$,100 μM ATP supplemented with various concentrations of $[P_2Mo_{18}O_{62}]^{6-}$ (c = 0 to 1000 nM, as indicated in Figure S2). For each experiment, samples were prepared in 50 μl of the previous buffer prior to loading by adding first CK2 then POM. Gradients were centrifuged at 4°C for 8 hr at 200,000 × g and were fractionated by pipetting 125 μl aliquots. For each condition, identical gradients were run by using horseradish peroxydase (3.5S) and β-galactosidase (12S) as sedimentation markers, which were detected by SDS-PAGE followed by silver staining.

Selectivity of the Polyoxometalate Inhibitor

To assess the degree of selectivity of the most effective POM, namely, $[P_2Mo_{18}O_{62}]^{6-}$, it was tested at 100 nM concentration for its ability to inhibit a panel of 29 recombinant protein kinases by using the Kinase Profiler Assay (Upstate). Final ATP concentration in the assay was 100 μM. IC_{50} values for selected kinases were determined by using a range of ten concentrations of $[P_2Mo_{18}O_{62}]^{6-}$.

Proteolysis Mapping

A sample of CK2α (90 μg) was diluted in 135 μl 50 mM Tris-HCl (pH 7.4), 150 mM NaCl and was incubated for 20 min at 23°C in the presence or absence of 63 μM $[P_2Mo_{18}O_{62}]^{6-}$. CK2α-$[P_2Mo_{18}O_{62}]^{6-}$ complexes were recovered by gel-filtration by using Biospin 6 chromatography columns (Biorad) according to the manufacturer's recommendations and were subjected to time course proteolysis in the presence of 0.9 μg trypsin. Protein fragments were resolved by 18% SDS-PAGE and Coomassie blue staining. Low-molecular weight fragments were extracted from the gel and subjected to protein sequence determination.

Protein Sequence Determination

Amino acid sequencing analysis was performed by using an Applied Biosystems gas-phase sequencer model 492. Phenylthiohydantoin amino acid derivatives generated at each sequencing cycle were identified and quantified on-line with an applied Biosystems Model 140C HPLC system. The procedures and reagents used were as recommended by the manufacturer. Retention times and integration values of peaks were compared to the chromatographic profile obtained for a standard mixture of derivatized amino acids.

Polyoxometalate-CK2α Binding Assay

Biotin-Keggin polyoxometalate (0.1 μM) or Biotin-CK2β (0.1 μM) were incubated for 30 min at 4°C with Streptavidin-agarose beads (Sigma). After washing in 50 mM Tris-HCl (pH 7.4), 150 mM NaCl, beads were incubated for 15 min at 4°C with CK2α (240 ng). The agarose beads were then centrifuged for 2 min at 14,000 rpm, and 3 μl supernatant was assayed for CK2 activity. The beads were washed in 50 mM Tris-HCl (pH 7.4), 150 mM NaCl, and the presence of CK2α associated to the beads was detected by western blot.

Construction of Plasmids Expressing CK2α Mutants and Protein Expression

CK2α mutants were obtained from the pET28-CK2α (full length)/GST-expressing plasmid (Filhol et al., 2003) by using the Quick change site-directed mutagenesis kit (Stratagene). The following primers were used:

5′-CGAAAATTAGGCCGAGGCGCATACTCTGAAGTACTTGAAGCC-3′ (K49A/F54L-forward),
5′-GGCTTCAAGTACTTCAGAGTATGCGCCTCGGCCTAATTTTCG-3′ (K49A/F54L-reverse),
5′-GTTAAAATTCTGAAGCCTGTTGCAAAGAAGAAAATCAAGCGTG-3′ (K74A-forward),
5′-CACGCTTGATTTTCTTCTTTGCAACAGGCTTCAGAATTTTAAC-3′ (K74A-reverse),
5′-GGAGTACAATGTCGCAGTGGCCTCGAGATATTTCAAAGGACC-3′ (R191A-forward), and
5′-GGTCCTTTGAAATATCTCGAGGCCACTGCGACATTGTACTCC-3′ (R191A-reverse).

All mutations were verified by DNA sequencing.

Wild-type and mutant CK2α were produced by using standard protein purification methods. Briefly, they were expressed in *Escherichia coli* BL21 (2 hr with 0.5 mM IPTG), and proteins were purified by using glutathione Sepharose beads (GE Healtcare). The retained fusion protein was cleaved by using 60 U thrombin (Sigma), and the CK2α proteins were then eluted in 50 mM Tris-HCl (pH 7.4) containing 150 mM NaCl, 2% glycerol, 1 mM DTT, and protease inhibitors. Proteins were quantified by a Bradford assay, and the quality of the purification was asserted by SDS-PAGE analysis.

Cellular CK2 Activity Assay

The assay will be described in detail elsewhere. Briefly, a CK2 activity reporter plasmid (pEYFPc1-SβS), which consists of several repeats of a CK2 peptide substrate fused to EYFP, was transfected in HeLa cells. Transfected cells were incubated for the indicated time with fresh medium containing the compounds. Then, 50 μg cellular proteins was resolved on a 12% native-polyacrylamide gel. After electrotransfer, the membrane was immunoblotted with the mAb anti-GFP (Roche), followed by incubation with a goat anti-mouse-HRP secondary antibody (Sigma), and YFP was revealed with the ECL plus western blot detection system (GE Healthcare).

SUPPLEMENTAL DATA

Supplemental Data three tables, four figures, and Supplemental Experimental Procedures and can be found with this article online at http://www.chembiol.com/cgi/content/full/15/7/683/DC1/.

ACKNOWLEDGMENTS

This work was supported by Institut National de la Santé et de la Recherche Médicale, Commissariat à l'énergie Atomique, the Ligue Nationale contre le Cancer (C.C. équipe labellisée 2007), the Institut National du Cancer (grant no. 57 to C.C.), Centre National Recherche Scientifique, Agence Nationale de la Recherche (grant JC05_41806 to B.H., E.L., S.T.), Université Pierre et Marie Curie (UPMC), Ministère de l'éducation Nationale, de la Recherche et Technologie, and Institut Universitaire de France. We thank the Drug Synthesis & Chemistry Branch, Developmental Therapeutics Program, Division of Cancer Treatment and Diagnosis, National Cancer Institute, for the library of low-molecular-weight compounds; Michael Pope (Georgetown University), René Thouvenot, and Géraldine Lenoble (UPMC) for providing us with samples

of POMs; and Jean-Pierre Andrieu (Institut de Biologie Structurale, Grenoble) for protein sequence determination. We also acknowledge very fruitful discussions with René Thouvenot.

Received: December 19, 2007
Revised: May 22, 2008
Accepted: May 27, 2008
Published: July 18, 2008

REFERENCES

Ahmed, K., Gerber, D.A., and Cochet, C. (2002). Joining the cell survival squad: an emerging role for protein kinase CK2. Trends Cell Biol. *12*, 226–230.

Aureliano, M., and Gandara, R.M.C. (2005). Decavanadate effects in biological systems. J. Inorg. Biochem. *99*, 979–985.

Bareyt, S., Piligkos, S., Hasenknopf, B., Gouzerh, P., Lacôte, E., Thorimbert, S., and Malacria, M. (2003). Highly efficient peptide bond formation to functionalized Wells-Dawson-type polyoxotungstates. Angew. Chem. Int. Ed. *42*, 3404–3406.

Bareyt, S., Piligkos, S., Hasenknopf, B., Gouzerh, P., Lacote, E., Thorimbert, S., and Malacria, M. (2005). Efficient preparation of functionalized hybrid organic/inorganic Wells-Dawson-type polyoxotungstates. J. Am. Chem. Soc. *127*, 6788–6794.

Bartis, J., Dankova, M., Blumenstein, M., and Francesconi, L.C. (1997). Preparation of lanthanide complexes of heteropolytungstates and characterization by ^{183}W and ^{31}P NMR spectroscopy. J. Alloy. Comp. *249*, 56–68.

Briand, L.E., Valle, G.M., and Thomas, H.J. (2002). Stability of the phosphomolybdic Dawson-type ion $[P_2Mo_{18}O_{62}]^{6-}$ in aqueous media. J. Mater. Chem. *12*, 299–304.

Bogoyevitch, M.A., and Fairlie, D.P. (2007). A new paradigm for protein kinase inhibition: blocking phosphorylation without directly targeting ATP binding. Drug Discov. Today *12*, 622–633.

Crans, D.C. (1993). Interactions of oxovanadates and selected oxomolybdates with enzymes. Mol. Eng. *3*, 277–284.

Contant, R. (1987). Comparative-study of tungstophosphates related to the $PW_{12}O_{40}^{3-}$ anion - synthesis and properties of $K_{10}P_2W_{20}O_{70}\cdot 24H_2O$, a new lacunary polyoxotungstophosphate. Can. J. Chem. *65*, 568–573.

Contant, R. (1990). Potassium octadecatungstodiphosphates(V) and related lacunary compounds. Inorg. Synth. *27*, 104–111.

Filhol, O., Cochet, C., Wedegaertner, P., Gill, G.N., and Chambaz, E.M. (1991). Coexpression of both α and β subunits is required for assembly of regulated casein kinase II. Biochemistry *30*, 11133–11140.

Filhol, O., Nueda, A., Martel, V., Gerber-Scokaert, D., Benitez, M.J., Souchier, C., Saoudi, Y., and Cochet, C. (2003). Live-cell fluorescence imaging reveals the dynamics of protein kinase CK2 individual subunits. Mol. Cell. Biol. *3*, 975–987.

Hasenknopf, B. (2005). Polyoxometalates: introduction to a class of inorganic compounds and their biomedical applications. Front. Biosci. *10*, 275–287.

Heriche, J.K., Lebrin, F., Rabilloud, T., Leroy, D., Chambaz, E.M., and Goldberg, Y. (1997). Regulation of protein phosphatase 2A by direct interaction with casein kinase 2α. Science *276*, 952–955.

Hervé, M., Sinoussi-Barre, F., Chermann, J.C., Hervé, G., and Jasmin, C. (1983). Correlation between structure of polyoxotungstates and their inhibitory activity on polymerases. Biochem. Biophys. Res. Commun. *116*, 222–229.

Hill, C.L., Weeks, M.S., and Schinazi, R.F. (1990). Anti-HIV-1 activity, toxicity, and stability studies of representative structural families of polyoxometalates. J. Med. Chem. *33*, 2767–2772.

Himeno, S., Hashimoto, M., and Ueda, T. (1999). Formation and conversion of molybdophosphate and arsenate complexes in aqueous solution. Inorg. Chim. Acta *284*, 237–245.

Hornstein, B.J., and Finke, R.G. (2002). The lacunary polyoxoanion synthon α-$[P_2W_{15}O_{56}]^{12-}$: an investigation of the key variables in its synthesis plus multiple control reactions leading to a reliable synthesis. Inorg. Chem. *41*, 2720–2730.

Hu, D., Shao, C., Guan, W., Su, Z., and Sun, J. (2007). Studies on the interactions of Ti-containing polyoxometalates (POMs) with SARS-CoV 3CLpro by molecular modeling. J. Inorg. Biochem. *101*, 89–94.

Judd, D.A., Nettles, J.H., Nevins, N., Snyder, J.P., Liotta, D.C., Tang, J., Ermolieff, J., Schinazi, R.F., and Hill, C.L. (2001). Polyoxometalate HIV-1 protease inhibitors. A new mode of protease inhibition. J. Am. Chem. Soc. *123*, 886–897.

Kim, J.S., Eom, J.I., Cheong, J.W., Choi, A.J., Lee, J.K., Yang, W.I., and Min, Y.H. (2007). Protein kinase CK2α as an unfavorable prognostic marker and novel therapeutic target in acute myeloid leukemia. Clin. Cancer Res. *13*, 1019–1028.

Klemperer, W.G. (1990). Tetrabutylammonium isopolyoxometalates. Inorg. Synth. *27*, 71–85.

Laramas, M., Pasquier, D., Filhol, O., Ringeisen, F., Descotes, J.L., and Cochet, C. (2007). Nuclear localization of protein kinase CK2 catalytic subunit (CK2α) is associated with poor prognostic factors in human prostate cancer. Eur. J. Cancer *43*, 928–934.

Lee, I.S., Long, J.R., Prusiner, S.B., and Sfar, J.G. (2005). Selective precipitation of prions by polyoxometalate complexes. J. Am. Chem. Soc. *127*, 13802–13803.

Litchfield, D.W. (2003). Protein kinase CK2: structure, regulation and role in cellular decisions of life and death. Biochem. J. *369*, 1–15.

Meggio, F., Pagano, M.A., Moro, S., Zagotto, G., Ruzzene, M., Sarno, S., Cozza, G., Bain, J., Elliott, M., Deana, A.D., et al. (2004). Inhibition of protein kinase CK2 by condensed polyphenolic derivatives. An in vitro and in vivo study. Biochemistry *43*, 12931–12936.

Mitsui, S., Ogata, A., Yanagie, H., Kasano, H., Hisa, T., Yamase, T., and Eriguchi, M. (2006). Antitumor activity of polyoxomolybdate, $(NH_3Pr^i)_6[Mo_7O_{24}]\cdot 3H_2O$, against, human gastric cancer model. Biomed. Pharmacother. *60*, 353–358.

Müller, C.E., Iqbal, J., Baqi, Y., Zimmermann, H., Röllich, A., and Stephan, H. (2006). Polyoxometalates-a new class of potent ecto-nucleoside triphosphate diphosphohydrolase (NTPDase) inhibitors. Bioorg. Med. Chem. Lett. *16*, 5943–5947.

Niefind, K., Guerra, B., Ermakowa, I., and Issinger, O.G. (2001). Crystal structure of human protein kinase CK2: insights into basic properties of the CK2 holoenzyme. EMBO J. *20*, 5320–5331.

Pagano, M.A., Meggio, F., Ruzzene, M., Andrzejewska, M., Kazimierczuk, Z., and Pinna, L.A. (2004). 2-Dimethylamino-4,5,6,7-tetrabromo-1H-benzimidazole: a novel powerful and selective inhibitor of protein kinase CK2. Biochem. Biophys. Res. Commun. *321*, 1040–1044.

Pagano, M.A., Cesaro, L., Meggio, F., and Pinna, L.A. (2006). Protein kinase CK2: a newcomer in the 'druggable kinome'. Biochem. Soc. Trans. *34*, 1303–1306.

Pettersson, L., Andersson, I., and Öhman, L.O. (1986). Multicomponent polyanions. 39. Speciation in the aqueous hydrogen ion-molybdate(MoO_4^{2-})-hydrogenphosphate(HPO_4^{2-}) system as deduced from a combined Emf-phosphorus-31 NMR study. Inorg. Chem. *25*, 4726–4733.

Pluskey, S., Mahroof-Tahir, M., Crans, D.C., and Lawrence, D.S. (1997). Vanadium oxoanions and cAMP-dependent protein kinase: an anti-substrate inhibitor. Biochem. J. *321*, 333–339.

Pope, M.T. (2003). Introduction to polyoxometalate chemistry. In Polyoxometalate Molecular Science, *Volume 98*, J.J. Borras-Almenar, E. Coronado, A. Müller, and M.T. Pope, eds. (Dordrecht: Kluwer Academic Publishers), pp. 3–31.

Rhule, J.T., Hill, C.L., Judd, D.A., and Schinazi, R.F. (1998). Polyoxometalates in medicine. Chem. Rev. *98*, 327–357.

Ruhlmann, L., Nadjo, L., Canny, J., Contant, R., and Thouvenot, R. (2002). Di- and tetranuclear Dawson-derived sandwich complexes: Synthesis, spectroscopic characterization, and electrochemical behavior. Eur. J. Inorg. Chem., 975–986.

Sarafianos, S.G., Kortz, U., Pope, M.T., and Modak, M.J. (1996). Mechanism of polyoxometalate-mediated inactivation of DNA polymerases: an analysis with HIV-1 reverse transcriptase indicates specificity for the DNA-binding cleft. Biochem. J. *319*, 619–626.

Sarno, S., Ghisellini, P., and Pinna, L.A. (2002). Unique activation mechanism of protein kinase CK2. The N-terminal segment is essential for constitutive activity of the catalytic subunit but not of the holoenzyme. J. Biol. Chem. *277*, 22509–22514.

Sarno, S., de-Moliner, E., Ruzzene, M., Pagano, M.A., Battistutta, R., Bain, J., Fabbro, D., Schoepfer, J., Elliott, M., Furet, P., et al. (2003). Biochemical and three-dimensional-structural study of the specific inhibition of protein kinase CK2 by [5-oxo-5,6-dihydroindolo-(1,2-a)quinazolin-7-yl]acetic acid (IQA). Biochem. J. *374*, 639–646.

Sazani, G., and Pope, M.T. (2004). Organotin and organogermanium linkers for simple, direct functionalization of polyoxotungstates. Dalton Trans. *Jul 7*, 1989–1994.

Schemberg, J., Schneider, K., Demmer, U., Warkentin, E., Müller, A., and Ermler, U. (2007). Towards biological supramolecular chemistry: a variety of pocket-templated, individual metal oxide cluster nucleations in the cavity of a Mo/W-storage protein. Angew. Chem. Int. Ed. Engl. *46*, 2408–2413 and 2970.

Sun, L., Wu, Q., Liu, N., Yang, C., Liu, L., Liu, Z., and Zhao, D. (2004). Effects of $K_5[SiW_{11}O_{39}Co]$ on mitogenic activity of basic fibroblast growth factor. Chem. Lett. (Jpn.) *33*, 298–299.

Tajima, Y. (2004). Anionic properties of polyoxometalates. Trends Inorg. Chem. *8*, 107–117.

Tawfic, S., Yu, S., Wang, H., Faust, R., Davis, A., and Ahmed, K. (2001). Protein kinase CK2 signal in neoplasia. Histol. Histopathol. *16*, 573–582.

Valero, E., Debonis, S., Filhol, O., Wade, R.H., Langowski, J., Chambaz, E.M., and Cochet, C. (1995). Quaternary structure of casein kinase-2 - characterization of multiple oligomeric states and relation with its catalytic activity. J. Biol. Chem. *270*, 8345–8352.

Vangrevelinghe, E., Zimmermann, K., Schoepfer, J., Portmann, R., Fabbro, D., and Furet, P. (2003). Discovery of a potent and selective protein kinase CK2 inhibitor by high-throughput docking. J. Med. Chem. *46*, 2656–2662.

Williams, D.S., Carroll, P.J., and Meggers, E. (2007). Platinum complex as a nanomolar protein kinase inhibitor. Inorg. Chem. *46*, 2944–2946.

Wu, Q., Wang, J., Zhang, L., Hong, A., and Ren, J. (2005). Molecular recognition of basic fibroblast growth factor by polyoxometalates. Angew. Chem. Int. Ed. *44*, 4048–4052.

Yamase, T. (2005). Anti-tumor, -viral, and -bacterial activities of polyoxometalates for realizing an inorganic drug. J. Mater. Chem. *15*, 4773–4782.

